# I/Q Imbalance in Two-Way AF Relaying: Performance Analysis and Detection Mode Switch

Jingya Li[†], Michail Matthaiou[⋆†], and Tommy Svensson[†]
[†]Department of Signals and Systems, Chalmers University of Technology, Gothenburg, Sweden
[⋆]School of Electronics, Electrical Engineering and Computer Science, Queen's University Belfast, Belfast, U.K.
Email: jingya.li@chalmers.se, m.matthaiou@qub.ac.uk, tommy.svensson@chalmers.se

***Abstract*—This paper studies the impact of in-phase and quadrature-phase imbalance (IQI) in two-way amplify-and-forward (AF) relaying systems. In particular, the effective signal-to-interference-plus-noise ratio (SINR) is derived for each source node, considering four different linear detection schemes, namely, uncompensated (Uncomp) scheme, maximal-ratio-combining (MRC), zero-forcing (ZF) and minimum mean-square error (MMSE) based schemes. For each proposed scheme, the outage probability (OP) is investigated over independent, non-identically distributed Nakagami-$m$ fading channels, and exact closed-form expressions are derived for the first three schemes. Based on the closed-form OP expressions, an adaptive detection mode switching scheme is designed for minimizing the OP of both sources. An important observation is that, regardless of the channel conditions and transmit powers, the ZF-based scheme should always be selected if the target SINR is larger than $3$ ($4.77$dB), while the MRC-based scheme should be avoided if the target SINR is larger than $0.38$ ($-4.20$dB).**

## I. Introduction

Relaying-assisted transmission can offer significant performance benefits to wireless networks, including extending network coverage, improving the system reliability and providing a homogenous quality of service over the communication area [1]. In standard unidirectional or one-way relaying, the spectral efficiency is inherently low since the transmission from the source to the destination occupies two phases (i.e., time slots). To tackle this problem, bidirectional or two-way relaying, which allows two sources to exchange data through a relay simultaneously within two phases, was proposed and studied in [2]–[4] among others.

The vast majority of works in the area of relaying adopt the classical assumption of ideal transceiver hardware [5]–[8]. However, in practice, due to the limited accuracy of the analog components and the up/down conversion operations at the transceivers, relaying systems always suffer from hardware impairments, e.g., phase noise, power amplifier nonlinearities, and IQI. In this paper, we elaborate on the impact of IQI, which refers to the phase and/or amplitude mismatch between the in-phase (I) and quadrature (Q) signals at the transmitter (TX) and receiver (RX) sides. Such imbalance results in an additional image-signal, leading to significant performance loss especially in high-rate systems [9].

To the best of our knowledge, up to now very few works have investigated the impact of IQI on relaying systems. In particular, the impact of IQI on one-way relaying was analytically investigated in [10]–[13], where analytical expressions for the average symbol error probability (SEP), OP and ergodic capacity were derived, considering different fading channel models. The literature on two-way relaying impaired by IQI is even more scarce. In this context, [14] elaborated on the effects of IQI at two sources in two-way AF relaying, where integral-based bounds on the average SEP were derived over Rayleigh fading channels. Moreover, a baseband compensation algorithm was proposed, which combines the received signal with its conjugate for data detection. However, [14] did not consider IQI at the relay, which is more prone to IQI, since the hardware of the low-cost relay nodes is most likely to be of low quality. Most recently, the effects of IQI at the relay node in two-way relaying were investigated in [15] and [16]. The results of [15] and [16] include the development of power allocation schemes that maximize the minimum SINR of two sources, along with lower bounds on the OP over independent, non-identically distributed Nakagami-$m$ fading channels. Note that [10]–[16] did not work out any detection mode switching method to balance the I/Q-induced interference power and the enhanced noise power, in order to further improve the outage performance.

Motivated by the above discussion, we hereafter characterize the performance of dual-hop two-way AF relaying systems, where IQI affects both the TX and RX front-ends of the *relay node*. First, the effective SINR is derived for each source node, considering four different linear detection schemes, namely, Uncomp, MRC-based, ZF-based and MMSE-based schemes. Then, exact analytical expressions for the OP are obtained for the first three detection schemes, considering independent, non-identically distributed Nakagami-$m$ fading channels. With the closed-form OP expressions in hand, an adaptive detection mode switching method is proposed to minimize the OP of both sources. We analytically show that IQI at the relay node results in an SINR ceiling effect for the Uncomp and the MRC-based schemes. Interestingly, it is observed that the MRC-based scheme has a lower SINR ceiling, compared to the Uncomp scheme. Moreover, both our analytical and numerical

This work was supported in part by the Swedish Governmental Agency for Innovation Systems (VINNOVA) within the VINN Excellence Center Chase, and the Swedish Research Council VR under the project 621-2009-4555 Dynamic Multipoint Wireless Transmission.

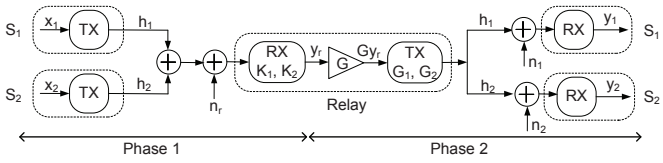


Fig. 1. Dual-hop two-way AF relaying with IQI at the relay node.

results show that, depending on the transmit powers and the values of the target SINR, different detection schemes should be selected to minimize the OP. In particular, when the target SINR value is above 3 (4.77dB), the system will always switch to the ZF-based detection scheme, while the MRC-based scheme should be avoided if the target SINR is larger than 0.38 ($-4.20$dB).

## II. System and Signal Model

We consider a two-way AF relaying system where two source nodes, $S_1$ and $S_2$, communicate with each other through a single relay node. All nodes are equipped with a single antenna, and transmission at all nodes is constrained to the half-duplex mode, i.e., no node can transmit and receive at the same time. The data transmission is carried out in two phases, as depicted in Fig. 1. In phase 1, $S_1$ and $S_2$ simultaneously transmit their information to the relay node. In phase 2, the relay amplifies the received signal and broadcasts it to both sources. The RF front-ends of the source and the destination are assumed to be perfect. In this paper, we focus on the impact of the IQI at the relay node, since it normally deploys lower-quality hardware.

### A. IQI Model

In general, IQI refers to as the phase and amplitude imbalance between the I and Q signal paths at the transceivers. Here, we consider an asymmetrical IQI model, where the I branch is assumed to be ideal and the errors are modeled in the Q branch [9], [17]. In the case of TX IQI, the baseband representation of the up-converted TX signal can be given as

$$\hat{x} = G_1 x + G_2^* x^* \tag{1}$$

where $x$ is the baseband TX signal under perfect TX I/Q matching. In turn, $G_1$, $G_2$ are given by

$$G_1 \triangleq \left(1 + g_T e^{j\phi_T}\right)/2 \text{ and } G_2 \triangleq \left(1 - g_T e^{-j\phi_T}\right)/2 \tag{2}$$

where $g_T$ and $\phi_T$ model the TX amplitude and phase mismatch, respectively. Regarding the RX IQI, the down-conversion of the RF RX signal is given by

$$\hat{y} = K_1 y + K_2 y^* \tag{3}$$

where $y$ denotes the down-converted baseband RX signal under perfect RX I/Q matching. The coefficients $K_1$ and $K_2$ are

$$K_1 \triangleq \left(1 + g_R e^{-j\phi_R}\right)/2 \text{ and } K_2 \triangleq \left(1 - g_R e^{j\phi_R}\right)/2 \tag{4}$$

where $g_R$ and $\phi_R$ denote the RX amplitude and phase mismatch, respectively. The $x^*$ and $y^*$ terms in (1) and (3) are often referred to as the mirror signals introduced by IQI [9]. The severity of TX IQI and RX IQI can be determined by the *image rejection ratios,* which are defined as $\mathtt{IRR}_T \triangleq |G_2|^2 / |G_1|^2$ and $\mathtt{IRR}_R \triangleq |K_2|^2 / |K_1|^2$ respectively [18]–[20]. It is noted that for perfect I/Q matching, these imbalance parameters reduce to $g_T = g_R = 1$ and $\phi_T = \phi_R = 0$; thus, in this case, we will have $G_1 = K_1 = 1$, $G_2 = K_2 = 0$ and $\mathtt{IRR}_T = \mathtt{IRR}_R = 0$.

### B. End-to-End SINR without IQI Compensation

Let $h_i$ denote the channel coefficient for the $S_i$-to-relay link for $i = 1, 2$. The complex Gaussian receiver noises at $S_1$, $S_2$, and the relay are distributed as $n_1 \sim \mathcal{CN}(0, N_1)$, $n_2 \sim \mathcal{CN}(0, N_2)$, and $n_r \sim \mathcal{CN}(0, N_r)$, respectively. We will now use the relationships (1) and (3) to derive the end-to-end SINR for each source, considering the two-phase, two-way AF relaying protocol. We assume that the channels between the sources and the relay are reciprocal, and remain constant during these two phases.

In phase 1, $S_1$ and $S_2$ simultaneously transmit their information to the relay node. Under RX I/Q mismatch, the baseband RX signal after down-conversion at the relay node, $y_r$, is

$$y_r = K_1 (h_1 x_1 + h_2 x_2 + n_r) + K_2 (h_1 x_1 + h_2 x_2 + n_r)^* \tag{5}$$

where $x_1, x_2 \in \mathbb{C}$ are the transmitted signals from the $S_1$ and $S_2$, with average transmit power $\mathbb{E}\left\{|x_1|^2\right\} = P_1$ and $\mathbb{E}\left\{|x_2|^2\right\} = P_2$, respectively. Here, the operator $\mathbb{E}\{\cdot\}$ stands for expectation. In phase 2, the relay node amplifies the received signal at baseband with an amplification factor $\mathtt{G}$, up-converts it to RF, and then broadcasts it to both sources. With TX IQI at the relay, the baseband RX signal at $S_i$ is

$$y_i = h_i \left(G_i (\mathtt{G} y_r) + G_j^* (\mathtt{G} y_r)^*\right) + n_i \tag{6}$$

where $j = \frac{2}{i}$ with $i = 1, 2$. Substituting (5) into (6), we can write the received signal at $S_i$ as

$$\begin{aligned} y_i = {} & \mathtt{G} A h_i^2 x_i + \mathtt{G} B |h_i|^2 x_i^* + \mathtt{G} A h_i h_j x_j + \mathtt{G} B h_i h_j^* x_j^* \\ & + \mathtt{G} A h_i n_r + \mathtt{G} B h_i n_r^* + n_i \end{aligned} \tag{7}$$

where

$$A \triangleq G_1 K_1 + G_2^* K_2^* \text{ and } B \triangleq G_1 K_2 + G_2^* K_1^*. \tag{8}$$

We assume that each source node $S_i$ has perfect instantaneous information of the channel between itself and the relay, $h_i$, $i = 1, 2$. This information is then forwarded to the relay. Let $P_r$ be the power of the transmitted signal at the output of the relay node. The variable amplification factor $\mathtt{G}$ can be selected at the relay node as

$$\mathtt{G} = \sqrt{\frac{P_r}{D\left(|\rho_1|^2 P_1 + |\rho_2|^2 P_2 + N_r\right)}} \tag{9}$$

where $\rho_i \triangleq |h_i|^2$ and

$$D \triangleq \left(|G_1|^2 + |G_2|^2\right)\left(|K_1|^2 + |K_2|^2\right). \tag{10}$$

The IQI parameters ($A$, $B$ and $D$) and the gain factor $\mathtt{G}$ are broadcasted from the relay to both sources. Recall that the channel $h_i$ is known at $S_i$, $i = 1, 2$. Therefore, each source can cancel the corresponding self-interference terms, i.e., $\mathtt{G}Ah_i^2 x_i + \mathtt{G}B\left|h_i\right|^2 x_i^*$ for $S_i$, such that

$$\tilde{y}_i = \mathtt{G}Ah_ih_jx_j + \mathtt{G}Bh_ih_j^*x_j^* + \mathtt{G}Ah_in_r + \mathtt{G}Bh_in_r^* + n_i. \quad (11)$$

Without IQI compensation and by treating the IQI-induced interference as noise, the end-to-end SINR at $S_i$ can be obtained as

$$\gamma_{i,\text{e2e}}^{\text{Uncomp}} = \frac{\rho_i\rho_jP_j}{\kappa\rho_i\rho_jP_j + (1+\kappa)\,\rho_iN_r + \frac{1}{|A|^2\mathtt{G}^2}N_i}. \quad (12)$$

In this paper, this detection scheme is named as the Uncomp scheme. The ratio $\kappa \triangleq |B|^2/|A|^2$ is referred to as the *joint image-leakage ratio* of the considered relaying system [13], [15]. Note that for the case of perfect I/Q matching at the relay node, we have $A = 1$, $B = 0$ and $\kappa = 0$. In practice, the value of $\kappa$ satisfies $0 < \kappa < 0.1$ [17].

## III. Linear Detection Schemes

In order to reduce the IQI effects in two-way AF relaying, in this section, we consider linear detection at each source $S_i$ by combining the signal $\tilde{y}_i$ with its conjugate $\tilde{y}_i^*$, such that

$$\hat{y}_i = w_{i,1}^*\tilde{y}_i + w_{i,2}^*\tilde{y}_i^* \quad (13)$$

where $w_{i,1}$ and $w_{i,2}$ are weighting complex coefficients to be designed for data detection at source $S_i$, $i = 1, 2$. Substituting (11) into (13), we get

$$\begin{aligned}\hat{y}_i = {} & \mathtt{G}\boldsymbol{w}_i^H\boldsymbol{a}_ih_jx_j + \mathtt{G}\boldsymbol{w}_i^H\boldsymbol{b}_ih_j^*x_j^* \\ & + \mathtt{G}\boldsymbol{w}_i^H\boldsymbol{a}_in_r + \mathtt{G}\boldsymbol{w}_i^H\boldsymbol{b}_in_r^* + w_{i,1}^*n_i + w_{i,2}^*n_i^*\end{aligned} \quad (14)$$

where $\boldsymbol{w}_i \triangleq \left[w_{i,1}^H, w_{i,2}^H\right]^H$, $\boldsymbol{a}_i \triangleq [A^*h_i^*, Bh_i]^H$ and $\boldsymbol{b}_i \triangleq [B^*h_i^*, Ah_i]^H$. Here, $(\cdot)^H$ denotes the conjugate transpose. Thus, the end-to-end SINR at $S_i$ becomes

$$\gamma_{i,\text{e2e}} = \frac{\left|\boldsymbol{w}_i^H\boldsymbol{a}_i\right|^2}{\left|\boldsymbol{w}_i^H\boldsymbol{b}_i\right|^2 + \frac{\mathtt{G}^2\left(\left|\boldsymbol{w}_i^H\boldsymbol{a}_i\right|^2 + \left|\boldsymbol{w}_i^H\boldsymbol{b}_i\right|^2\right)N_r + \left\|\boldsymbol{w}_i^H\right\|^2N_i}{\mathtt{G}^2\rho_jP_j}}. \quad (15)$$

Without loss of generality, we assume that $\|\boldsymbol{w}_i\| = 1$ for $i = 1, 2$. Based on the selection of $\boldsymbol{w}_i$, in the following, we present three different linear detection schemes.

### A. MRC-based Scheme

The MRC-based detection scheme tries to maximize the received SNR, by ignoring the IQI-induced interference. The signal $\tilde{y}_i$ and its conjugate $\tilde{y}_i^*$ are co-phased such that the useful signals add up coherently. The complex weighted coefficients are selected as [21, Eq. (3.33)]

$$\boldsymbol{w}_i^{\text{MRC}} = \boldsymbol{a}_i/\left\|\boldsymbol{a}_i\right\|. \quad (16)$$

Substituting $\boldsymbol{w}_i^{\text{MRC}}$ and (9) into (15), the end-to-end SINR can be obtained as

$$\gamma_{i,\text{e2e}}^{\text{MRC}} = \frac{\rho_i\rho_jP_j}{\frac{4\kappa}{(1+\kappa)^2}\rho_i\rho_jP_j + \rho_i\left(1 + \frac{4\kappa}{(1+\kappa)^2}\right)N_r + \frac{1}{|A|^2\mathtt{G}^2(1+\kappa)}N_i}. \quad (17)$$

Comparing (17) with (12), we see that the MRC-based scheme can reduce the noise power from source $S_i$ by a factor of $(1+\kappa)$. However, this is achieved at a cost of increasing IQI-induced interference with a factor of $\frac{4}{(1+\kappa)^2}$. Thus, this detection scheme is more efficient for the noise-limited regime.

### B. ZF-based Scheme

The ZF based detection scheme aims to completely cancel the IQI-induced interference by choosing [21, Eq. (3.100)]

$$\boldsymbol{w}_i^{\text{ZF}} = \frac{1}{\sqrt{\left(|A|^2 + |B|^2\right)\rho_i}}\left[A^*h_i^*, -Bh_i\right]^H \quad (18)$$

yielding $\boldsymbol{w}_i^H\boldsymbol{b}_i = 0$. The end-to-end SINR in (15) becomes[1]

$$\gamma_{i,\text{e2e}}^{\text{ZF}} = \frac{\rho_i\rho_jP_j}{\rho_iN_r + \frac{1+\kappa}{|1-\kappa|^2|A|^2\mathtt{G}^2}N_i}. \quad (19)$$

Comparing (19) with (12), we see that by applying the ZF-based scheme, the IQI-induced interference has been completely eliminated. However, from (19), we see that the noise power from the source $S_i$ is increased by $\frac{1+\kappa}{|1-\kappa|^2}$ - a phenomenon known as noise enhancement for ZF-type of transformations [22]. Therefore, the ZF-based detection scheme is more efficient for IQI-limited systems.

### C. MMSE-based Scheme

The MMSE-based detection scheme provides the optimal linear IQI compensation that maximizes the end-to-end SINR. Define the full-rank matrix

$$\mathbf{R}_i \triangleq \boldsymbol{b}_i\boldsymbol{b}_i^H + \frac{N_r}{\rho_jP_j}\left(\boldsymbol{a}_i\boldsymbol{a}_i^H + \boldsymbol{b}_i\boldsymbol{b}_i^H\right) + \frac{N_i}{\mathtt{G}^2\rho_jP_j}\mathbf{I}_2. \quad (20)$$

Then, the SINR expression in (15) can be rewritten as a generalized Rayleigh quotient, $\gamma_{i,\text{e2e}} = \frac{\boldsymbol{w}_i^H\boldsymbol{a}_i\boldsymbol{a}_i^H\boldsymbol{w}_i}{\boldsymbol{w}_i^H\mathbf{R}_i\boldsymbol{w}_i}$, which is maximized by selecting [21, Eq. (8.61)]

$$\boldsymbol{w}_i^{\text{MMSE}} = \frac{\mathbf{R}_i^{-1}\boldsymbol{a}_i}{\left\|\mathbf{R}_i^{-1}\boldsymbol{a}_i\right\|}. \quad (21)$$

The corresponding maximum end-to-end SINR is

$$\gamma_{i,\text{e2e}}^{\text{MMSE}} = \boldsymbol{a}_i^H\mathbf{R}_i^{-1}\boldsymbol{a}_i = \frac{\rho_i\rho_jP_j + \rho_iN_r + \frac{(1+\kappa)N_i}{|1-\kappa|^2|A|^2\mathtt{G}^2}}{\rho_iN_r\left(1 + \frac{N_r}{\rho_jP_j}\right) + \mathcal{J}} \quad (22)$$

where

$$\mathcal{J} \triangleq \frac{(1+\kappa)\,N_i}{|1-\kappa|^2\,|A|^2\,\mathtt{G}^2}\left(1 + \frac{2N_r}{\rho_jP_j} + \frac{N_i}{|A|^2\,\mathtt{G}^2\,(1+\kappa)\,\rho_i\rho_jP_j}\right).$$

*Remark 1:* Compared to the MRC and ZF-based schemes, the MMSE-based scheme has a higher computational complexity, since it requires matrix inverse calculations to obtain the compensation vector $\boldsymbol{w}_i^{\text{MMSE}}$. Moreover, for the MMSE-based scheme, each source node $S_i$ needs to have instantaneous channel state information (CSI) of both $h_1$ and $h_2$ in

[1]Note that in practice, we have $\kappa < 0.1$, thus, $|1-\kappa|^2 \neq 0$, and the received SINR in (19) is always defined.

order to construct the matrix $\mathbf{R}_i$. On the contrary, for the MRC and ZF-based schemes, only local instantaneous CSI is required, that is, $S_i$ only needs to have the instantaneous information of the channel between itself and the relay, i.e., $h_i$. Therefore, the MMSE-based scheme also requires more channel knowledge. For the case of perfect IQ matching at the relay node (i.e., $\kappa = 0$), the received SINRs in (12), (17), (19) and (22) reduce all to the standard expression [3]

$$\gamma_{i,\text{e2e}}^{\text{ideal}} = \frac{\rho_i \rho_j P_j}{\rho_i N_r + \frac{1}{\mathtt{G}^2} N_i}. \tag{23}$$

## IV. Adaptive Detection Mode Switch

In this section, we propose an adaptive detection mode switching method, which minimizes the OPs of both sources. We start by deriving the OP expressions for the considered detection schemes. Since the OP performance analysis for the MMSE-based scheme is challenging, if not impossible, we hereafter focus on the Uncomp, MRC-based and ZF-based schemes.

### A. Outage Probability Analysis

The amplitudes $|h_1|$ and $|h_2|$ are modeled as independent, non-identical Nakagami-$m$ random variables with fading parameters $m_i \geq 0.5$, and average powers $\Omega_i = \mathbb{E}\left\{|h_i|^2\right\}$ for $i = 1, 2$. Therefore, $\rho_i \triangleq |h_i|^2$ is a Gamma random variable distributed with shape parameter $m_i$ and scale parameter $\dfrac{\Omega_i}{m_i}$. The OP at $S_i$, $i = 1, 2$, is defined as the probability that its instantaneous equivalent SINR, $\gamma_i$, falls below a certain threshold $\gamma_{\text{th}}$, that is,[2]

$$P_{\text{out},i}(\gamma_{\text{th}}) = \Pr\left\{\gamma_i \leq \gamma_{\text{th}}\right\} \tag{24}$$

where $\Pr\{\cdot\}$ denotes probability.

For convenience, we denote $\bar{\gamma}_i \triangleq P_i/N_r$ and $\bar{\gamma}_{r,i} \triangleq P_r/N_i$ for $i = 1, 2$. Substituting (9) into (12), (17) and (19), the received SINRs at $S_i$ for the uncompensated case and the cases with MRC and ZF-based compensation can be written in a general form as

$$\gamma_{i,\text{e2e}} = \frac{a_i \rho_i \rho_j}{b_i \rho_i \rho_j + c_i \rho_i + d_i \rho_i + 1} \tag{25}$$

where $j \triangleq \frac{2}{i}$ for $i = 1, 2$. The positive values $a_i, c_i, d_i$ and non-negative value $b_i$ are given in Table I, where $\alpha^{\text{ZF}} \triangleq \frac{|1-\kappa|^2 |A|^2}{(1+\kappa)D}$. Based on the received SNR expression in (25), we present the following exact closed-from OP expression.

*Proposition 1:* For Nakagami-$m$ fading channels with integer $m_i$, the OPs at $S_i$ for the Uncomp and the MRC-based schemes can be expressed as

Table I
SINR parameters

| | Uncomp | MRC-based | ZF-based |
|---|---|---|---|
| $a_i$ | $\frac{\lvert A\rvert^2}{D}\bar{\gamma}_j\bar{\gamma}_{r,i}$ | $\frac{(1+\kappa)\lvert A\rvert^2}{D}\bar{\gamma}_j\bar{\gamma}_{r,i}$ | $\alpha^{\text{ZF}}\bar{\gamma}_j\bar{\gamma}_{r,i}$ |
| $b_i$ | $\frac{\kappa\lvert A\rvert^2}{D}\bar{\gamma}_j\bar{\gamma}_{r,i}$ | $\frac{4\kappa\lvert A\rvert^2}{(1+\kappa)D}\bar{\gamma}_j\bar{\gamma}_{r,i}$ | 0 |
| $c_i$ | $\frac{\lvert A\rvert^2(1+\kappa)\bar{\gamma}_{r,i}}{D} + \bar{\gamma}_i$ | $\frac{\left(1+6\kappa+\kappa^2\right)\lvert A\rvert^2\bar{\gamma}_{r,i}}{(1+\kappa)D} + \bar{\gamma}_i$ | $\alpha^{\text{ZF}}\bar{\gamma}_{r,i} + \bar{\gamma}_i$ |
| $d_i$ | $\bar{\gamma}_j$ | $\bar{\gamma}_j$ | $\bar{\gamma}_j$ |

$$\begin{aligned} P_{\text{out},i}(\gamma_{\text{th}}) = 1 &- \frac{2}{\Gamma(m_i)}\left(\frac{m_i}{\Omega_i}\right)^{m_i} \exp\left(-\frac{m_i\tilde{\gamma}_i}{\Omega_i} - \frac{c_i\tilde{\gamma}_i m_j}{d_i\Omega_j}\right) \\ &\times \sum_{k=0}^{m_j-1}\sum_{l=0}^{k}\sum_{\nu=0}^{m_i-1}\frac{1}{k!}\left(\frac{c_i m_j}{d_i\Omega_j}\right)^k \binom{k}{l}\binom{m_i-1}{\nu} \\ &\times \tilde{\gamma}_i^{k+m_i-\nu-1}\left(\tilde{\gamma}_i + \frac{1}{c_i}\right)^{k-l} \\ &\times \left(\frac{\left(c_i\tilde{\gamma}_i+1\right)\tilde{\gamma}_i m_j\Omega_i}{d_i m_i\Omega_j}\right)^{\frac{l+\nu-k+1}{2}} \\ &\times K_{l+\nu-k+1}\left(2\sqrt{\frac{\left(c_i\tilde{\gamma}_i+1\right)\tilde{\gamma}_i m_i m_j}{d_i\Omega_i\Omega_j}}\right) \end{aligned} \tag{26}$$

for $0 \leq \gamma_{\text{th}} < \frac{a_i}{b_i}$, and $P_{\text{out},i}(\gamma_{\text{th}}) = 1$ for $\gamma_{\text{th}} \geq \frac{a_i}{b_i}$, $i = 1, 2$. Here, $\tilde{\gamma}_i \triangleq \frac{d_i\gamma_{\text{th}}}{a_i - b_i\gamma_{\text{th}}}$. Also, $\Gamma(x) = \int_0^\infty t^{x-1}\exp(-t)\,dt$ is the Gamma function, and $K_v(\cdot)$ is the $v$-th order modified Bessel function of the second kind. For the ZF-based scheme, the SINR ceiling vanishes and the OP at $S_i$ is given as in (26) for all $\gamma_{\text{th}} \geq 0$, where $\tilde{\gamma}_i \triangleq \frac{d_i}{a_i}\gamma_{\text{th}}$.

*Proof:* See Appendix I. ∎

Proposition 1 shows that, due to the effect of IQI, the OP at each source node is always 1 if $\gamma_{\text{th}} \geq \frac{1}{\kappa}$ for the Uncomp scheme, and if $\gamma_{\text{th}} \geq \frac{(1+\kappa)^2}{4\kappa}$ for the MRC-based scheme. The values $\frac{1}{\kappa}$ and $\frac{(1+\kappa)^2}{4\kappa}$ can be regarded as the SINR ceilings in the high SNR regime, caused by IQI at the relay [13], [23], [24]. This implies that, for the Uncomp and MRC-based schemes, outage will always happen if the target SINR threshold is above their corresponding SINR ceilings. Note that in practice, we have $0 < \kappa < 0.1$, thus, $\frac{1}{\kappa} > \frac{(1+\kappa)^2}{4\kappa}$, i.e., the MRC-based scheme has a lower SINR ceiling, compared to the Uncomp scheme. This implies that, in the high SNR regime, the MRC-based detection performs worse than the Uncomp scheme. This result, though unexpected, makes very good sense because in the high SNR regime, the system becomes IQI-limited, and the MRC-based scheme increases the IQI-induced interference (Section III-A). From Proposition 1, we also observe that the ZF-based compensation scheme does not have the SINR ceiling effect, since the IQI-induced interference is completely canceled. However, as discussed in Section III-B, this IQI compensation scheme enhances the

[2]The value of $\gamma_{\text{th}}$ is usually predefined in order to satisfy a certain quality-of-service requirement, e.g., to achieve $\log_2(1+\gamma_{\text{th}})$ bits/channel use.

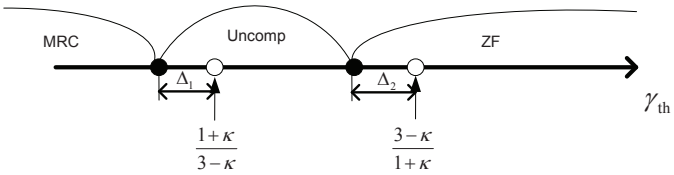


Fig. 2. Adaptive detection mode switch for two-way relaying.

noise power. Thus, the ZF-based scheme should be avoided when the system is noise-limited.

### B. Adaptive Mode Switch

Let $P_{\text{out},i}^{\text{Uncomp}}(\gamma_{\text{th}})$, $P_{\text{out},i}^{\text{MRC}}(\gamma_{\text{th}})$ and $P_{\text{out},i}^{\text{ZF}}(\gamma_{\text{th}})$ denote the OPs for the Uncomp, MRC-based and ZF-based schemes, respectively. Based on the derived exact OP expression in (26), we now present the following insightful guidelines for the design of adaptive compensation mode switch:

*Proposition 2:* For Nakagami-$m$ fading channels with integer $m_i$, we always have

1) $P_{\text{out},i}^{\text{MRC}}(\gamma_{\text{th}}) > P_{\text{out},i}^{\text{Uncomp}}(\gamma_{\text{th}})$ if $\gamma_{\text{th}} \geq \frac{1+\kappa}{3-\kappa}$;
2) $P_{\text{out},i}^{\text{Uncomp}}(\gamma_{\text{th}}) > P_{\text{out},i}^{\text{ZF}}(\gamma_{\text{th}})$ if $\gamma_{\text{th}} \geq \frac{3-\kappa}{1+\kappa}$.

Here, $\kappa$ is the joint image-leakage ratio defined in Section II-B, with $0 < \kappa < 0.1$ in practice.

*Proof:* See Appendix II. ∎

Proposition 2 implies that, depending on the value of the target SINR $\gamma_{\text{th}}$, different detection schemes should be selected to minimize the OPs. Based on Proposition 2 and notice that $\frac{1+\kappa}{3-\kappa} < \frac{3-\kappa}{1+\kappa}$ for $0 < \kappa < 0.1$, the optimal model switch between the Uncomp, MRC-based and ZF-based schemes can be interpreted in Fig. 2. We see that the optimal switching point between the MRC-based scheme and the Uncomp scheme is $\frac{1+\kappa}{3-\kappa} - \Delta_1$, while $\frac{3-\kappa}{1+\kappa} - \Delta_2$ is the optimal switching point between the Uncomp scheme and the ZF-based scheme. The differences, $\Delta_1$ and $\Delta_2$ are caused due to the fact that different schemes have different values of $c_i$.

From Table I, we see that when the transmit SNRs of the relay-to-source links is much less than the transmit SNRs of the source-to-relay links (i.e., $\bar{\gamma}_{r,i} \ll \bar{\gamma}_i$), the differences between the values of $c_i$ are negligible. In these cases, the values of $\Delta_1$ and $\Delta_2$ converge to 0. Then, the two points $\gamma_{\text{th}} = \frac{1+\kappa}{3-\kappa}$ and $\gamma_{\text{th}} = \frac{3-\kappa}{1+\kappa}$ become very close to the mode switching points. As $\bar{\gamma}_{r,i} - \bar{\gamma}_i$ increases, the differences between the values of $c_i$ for different schemes increase. Then, $\Delta_1$ and $\Delta_2$ become the dominating terms that affect the optimal switching points. When $\bar{\gamma}_{r,i} \gg \bar{\gamma}_i$, the two switching points will disappear, and the ZF-based scheme will always outperform the other two schemes.

Moreover, note that $\frac{1+\kappa}{3-\kappa} < 0.38$ and $\frac{3-\kappa}{1+\kappa} < 3$ for $0 < \kappa < 0.1$. Then, we have the following corollary:

*Corollary 1:* Regardless of the channel conditions and transmit SNRs, the ZF-based scheme should always be selected if $\gamma_{\text{th}} \geq 3$ (4.77dB), and the MRC-based scheme should be avoided if $\gamma_{\text{th}} \geq 0.38$ (−4.20dB).

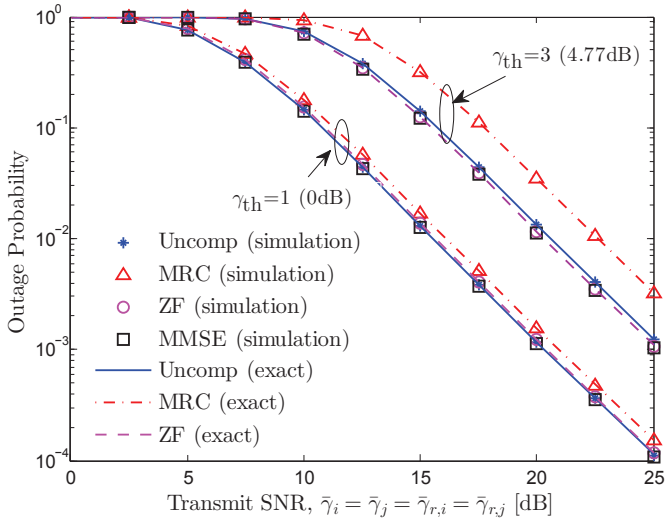


Fig. 3. Outage probability vs. transmit SNRs. The channel fading parameters are $m_1 = m_2 = 2$ and $\Omega_1 = \Omega_2 = 1$.

## V. Numerical Results

In this section, we present a set of numerical results to evaluate the performance of the proposed adaptive mode switching scheme and to verify our analytical results. Figure 3 shows the OP at each source node as a function of the transmit SNR. The exact analytical expression (26) is compared with Monte-Carlo simulations for different detection schemes. The simulated OP with the MMSE-based scheme is also depicted for comparative purposes. We consider symmetric IQI at the relay node with TX and RX image rejection ratios given as $\text{IRR}_T = \text{IRR}_R \approx -20$dB, which correspond to $20\log_{10}(g_T) = 20\log_{10}(g_R) = 1.58$dB amplitude imbalance and $\phi_T = \phi_R = 5°$ phase imbalance. The joint image rejection ratio of the system is $\kappa = 0.04$. As can be seen, the exact analytical OP expression agrees perfectly with the numerical results. In agreement with Corollary 1, we observe that when $\gamma_{\text{th}} = 3$ (4.77dB), the ZF-based scheme achieves the lowest OP over the entire range of SNRs, compared to the Uncomp and the MRC-based schemes. Moreover, as anticipated, the MRC-based scheme has the worst performance for both $\gamma_{\text{th}} = 3$ (4.77dB) and $\gamma_{\text{th}} = 1$ (0dB), since $\gamma_{\text{th}} > 0.38$ (−4.20dB) for both cases.

Figure 4 demonstrates the OP of the two sources versus the target SINR $\gamma_{\text{th}}$, for $0.05 \leq \gamma_{\text{th}} \leq 0.5$ and considering the same IQI parameters used in Fig. 3. We see that for the case where the transmit SNRs of the relay-to-source links is much less than the transmit SNRs of the source-to-relay links (i.e., $\bar{\gamma}_i = \bar{\gamma}_j = 15$dB, $\bar{\gamma}_{r,i} = \bar{\gamma}_{r,j} = 5$dB), there is a switching point between the MRC-based scheme and the Uncomp scheme. The value of $\gamma_{\text{th}}$ corresponding to the switching point is around $\frac{1+\kappa}{3-\kappa} \approx 0.35$ , which is in agreement with Proposition 2. As expected, this switching point moves towards left and then disappears as $\bar{\gamma}_{r,i}$ and $\bar{\gamma}_{r,j}$ increase. We also observe that, for the low target SINRs ($0.05 \leq \gamma_{\text{th}} \leq 0.5$), the ZF-based scheme performs the worst for the two cases when $\bar{\gamma}_{r,i} = \bar{\gamma}_{r,j} = 5$dB and $\bar{\gamma}_{r,i} = \bar{\gamma}_{r,j} = 10$dB. This is expected because in both

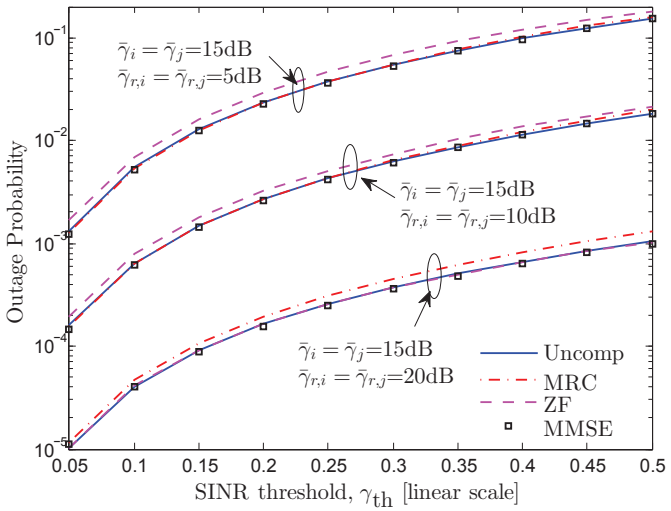


Fig. 4. Outage probability vs. SINR threshold $\gamma_{\text{th}}$. The channel fading parameters are $m_1 = m_2 = 2$ and $\Omega_1 = \Omega_2 = 1$.

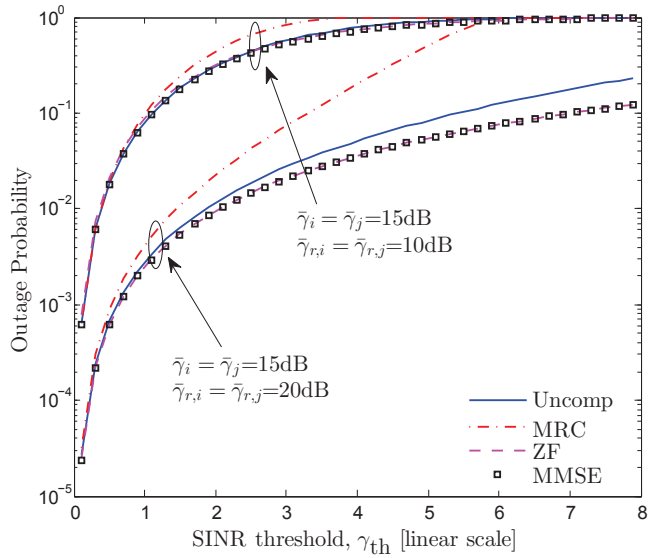


Fig. 5. Outage probability vs. SINR threshold $\gamma_{\text{th}}$. The channel fading parameters are $m_1 = m_2 = 2$ and $\Omega_1 = \Omega_2 = 1$.

cases, the OP is dominated by the value of $\tilde{\gamma}_i$ for all schemes. Over the considered range of $\gamma_{\text{th}}$, the ZF-based scheme has the largest $\tilde{\gamma}_i$, thus, resulting in the worst outage performance. Similar behavior for the mode switching between the Uncomp scheme and the ZF-based scheme can be seen in Fig. 5.

From Fig. 5 we see that the OP becomes equal to 1 for the MRC-based scheme once the SNR threshold, $\gamma_{\text{th}}$, reaches its SINR ceiling, i.e., $\frac{(1+\kappa)^2}{4\kappa} \approx 6.78$. This implies that the system is in full outage due to the effect of IQI, which cannot be avoided by improving the transmit SNRs [13], [23], [24]. The ceiling effect of the Uncomp scheme can also been seen if $\gamma_{\text{th}} \geq \frac{1}{\kappa} \approx 25.1$ (14dB). Note that comparing to the Uncomp scheme, the performance gain achieved by selecting the MRC-based scheme at low SINR thresholds is negligible. Therefore, an alternative mode switching method would be to remove the first switch point in Fig. 2, and only switch between the Uncomp and the ZF-based schemes.

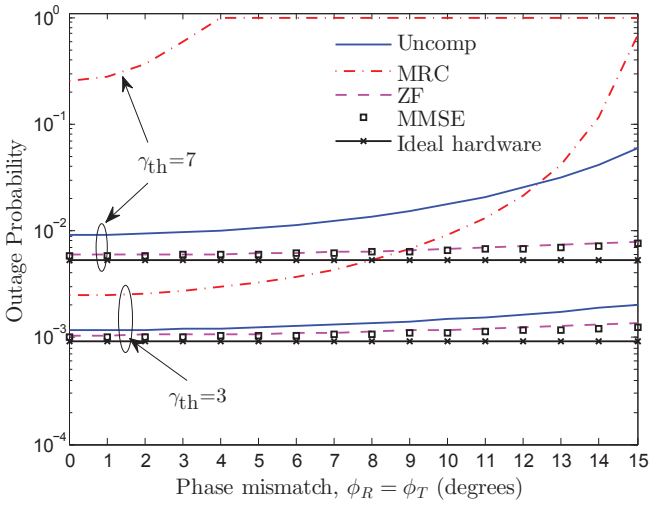


Fig. 6. Outage probability vs. the phase mismatch parameter $\phi_T = \phi_R$. The channel fading parameters are $m_1 = m_2 = 2$ and $\Omega_1 = \Omega_2 = 1$. The transmit SNRs are $\bar{\gamma}_i = \bar{\gamma}_j = \bar{\gamma}_{r,i} = \bar{\gamma}_{r,j} = 25$dB.

Finally, we investigate the impact of IQI on the outage performance for different detection schemes. The ideal hardware case is used as our performance baseline. Figure 6 shows the OP as a function of the phase mismatch, with the same amplitude imbalance parameters used in Fig. 3. We consider two target SINR thresholds, i.e., $\gamma_{\text{th}} = 3$ (4.77dB) and $\gamma_{\text{th}} = 7$ (8.45dB), in order to achieve 2bits/channel use and 3bits/channel use, respectively. As expected, the ZF-based scheme outperforms the Uncomp and MRC-based schemes over the entire range of the phase imbalance, since $\gamma_{\text{th}} \geq 3$ (4.77dB). Therefore, the ZF-based scheme should be selected for both cases. Moreover, we see that the Uncomp and the MRC-based schemes are very sensitive to the IQI levels at the relay, especially when the target SINR is high. On the contrary, the ZF-based scheme is more robust to the IQI effects, and it performs very close to the optimal MMSE-based scheme for both cases. We also observe that, compared to the Uncomp scheme and the MRC-based scheme, the performance gain achieved by the ZF-based scheme increases significantly as $\gamma_{\text{th}}$ increases. This implies that IQI cancellation plays an important role for reducing the OP for high data-rate systems.

## VI. Conclusions

In this paper, the performance of two-way AF relaying in the presence of IQI at the relay node was analyzed with different detection schemes at sources. More specifically, considering Nakagami-$m$ fading, closed-from OP expressions have been derived for the Uncomp, MRC and ZF-based detection schemes. Our theoretical analysis indicated that, for the Uncomp and MRC-based schemes, IQI at the relay node results in an SINR ceiling effect, which depends merely on the IQI parameter. Furthermore, an adaptive detection mode switching method was proposed to reduce the OP over all target SINRs. Compared to the Uncomp and MRC-based schemes, it is always better to select the ZF-based detection scheme when the target SINR is above 3 (4.77dB). Then, depending on the transmit SNRs of the relay-to-source and the

source-to-relay links, the system may switch to the Uncomp scheme, as the target SINR decreases.

## APPENDIX I
## PROOF OF PROPOSITION 1

Let $p_{\rho_i}(x)$ and $F_{\rho_i}(x)$ denote the PDF and CDF of $\rho_i$, respectively, for $i = 1, 2$. Plugging (25) into (24), the OP at $S_i$ becomes $P_{\text{out},i}(\gamma_{\text{th}}) = \Pr\left\{\frac{a_i\rho_i\rho_j}{b_i\rho_i\rho_j + c_i\rho_i + d_i\rho_i + 1} \leq \gamma_{\text{th}}\right\}$. If $b_i \neq 0$, then, we have $\gamma_{i,\text{e2e}} < \frac{a_i}{b_i}$. Thus, $P_{\text{out},i}(\gamma_{\text{th}}) = 1$ for $\gamma_{\text{th}} \geq \frac{a_i}{b_i}$. When $0 \leq \gamma_{\text{th}} < \frac{a_i}{b_i}$, the OP can be rewritten as

$$P_{\text{out},i}(\gamma_{\text{th}}) = \mathbb{E}_{\rho_i}\left\{\Pr\left\{\left(\rho_i - \tilde{\gamma}\right)\rho_j \leq \frac{\tilde{\gamma}_i\left(c_i\rho_i + 1\right)}{d_i}\middle|\, \rho_i\right\}\right\} \tag{27}$$

where $\tilde{\gamma}_i \triangleq \frac{d_i\gamma_{\text{th}}}{a_i - b_i\gamma_{\text{th}}}$. Note that

$$\Pr\left\{\left(\rho_i - \tilde{\gamma}\right)\rho_j \leq \frac{\tilde{\gamma}_i\left(c_i\rho_i + 1\right)}{d_i}\middle|\, \rho_i\right\} = \begin{cases} 1, & 0 \leq \rho_i \leq \tilde{\gamma}_i, \\ F_{\rho_j}\left(\frac{\tilde{\gamma}_i(c_i\rho_i+1)}{d_i(\rho_i - \tilde{\gamma}_i)}\right), & \rho_i \geq \tilde{\gamma}_i. \end{cases} \tag{28}$$

Hence, (27) can be further expressed as

$$P_{\text{out},i}(\gamma_{\text{th}}) = \int_0^{\tilde{\gamma}_i} 1 \cdot p_{\rho_i}(\rho_i)d\rho_i + \int_{\tilde{\gamma}_i}^{\infty} F_{\rho_j}\left(\frac{\tilde{\gamma}_i\left(c_i\rho_i + 1\right)}{d_i\left(\rho_i - \tilde{\gamma}_i\right)}\right) p_{\rho_i}(\rho_i)d\rho_i.$$

The result in (26) can then obtained by following the same methodology used in [13, Appendix II].

## APPENDIX II
## PROOF OF COROLLARY 1

Note that $\gamma_{i,\text{e2e}}$ in (25) is a monotonically decreasing function of $c_i$. Thus, $P_{\text{out},i}(\gamma_{\text{th}})$ increases as $c_i$ increases for all cases. Also, $\tilde{\gamma}_i$ defined in Proposition 1 is a monotonically increasing function of $\gamma_{\text{th}}$ for each case. Thus, we can show that $P_{\text{out},i}(\gamma_{\text{th}})$ in (26) increases as $\tilde{\gamma}_i$ increases. Let $c_i^{\text{Uncomp}}$, $c_i^{\text{MRC}}$ and $c_i^{\text{ZF}}$ denote the values of $c_i$ for the Uncomp, MRC-based and ZF-based schemes, respectively. Similarly, let $\tilde{\gamma}_i^{\text{Uncomp}}$, $\tilde{\gamma}_i^{\text{MRC}}$ and $\tilde{\gamma}_i^{\text{ZF}}$ denote the corresponding values of $\tilde{\gamma}_i$ for these different schemes. From Table I, it is easy to show that $c_i^{\text{ZF}} < c_i^{\text{Uncomp}} < c_i^{\text{MRC}}$ for $0 < \kappa < 1$. Moreover, we have

$$\frac{\tilde{\gamma}_i^{\text{MRC}}}{\tilde{\gamma}_i^{\text{Uncomp}}} = \frac{1 - \kappa\gamma_{\text{th}}}{1 + \kappa - \frac{4\kappa}{1+\kappa}\gamma_{\text{th}}} \tag{29}$$

and

$$\frac{\tilde{\gamma}_i^{\text{Uncomp}}}{\tilde{\gamma}_i^{\text{ZF}}} = \frac{|1 - \kappa|^2}{(1 + \kappa)(1 - \kappa\gamma_{\text{th}})}. \tag{30}$$

Therefore, if $\gamma_{\text{th}} \geq \frac{1+\kappa}{3-\kappa}$, then, from (29), we get $\tilde{\gamma}_i^{\text{MRC}} \geq \tilde{\gamma}_i^{\text{Uncomp}}$. Note that $\frac{1+\kappa}{3-\kappa}$ is smaller than the SINR ceilings of the Uncomp and MRC-based schemes, i.e., $\frac{1}{\kappa}$ and $\frac{(1+\kappa)^2}{4\kappa}$, respectively. Now, recall that $c_i^{\text{Uncomp}} < c_i^{\text{MRC}}$ and $P_{\text{out},i}(\gamma_{\text{th}})$ increases as $c_i$ or $\tilde{\gamma}_i$ increases. Thus, if $\gamma_{\text{th}} \geq \frac{1+\kappa}{3-\kappa}$, we have $P_{\text{out},i}^{\text{MRC}}(\gamma_{\text{th}}) > P_{\text{out},i}^{\text{Uncomp}}(\gamma_{\text{th}})$. Similarly, we can prove that $P_{\text{out},i}^{\text{Uncomp}}(\gamma_{\text{th}}) > P_{\text{out},i}^{\text{ZF}}(\gamma_{\text{th}})$ if $\gamma_{\text{th}} \geq \frac{3-\kappa}{1+\kappa}$.

## REFERENCES


[1] C. Hoymann, W. Chen, J. Montojo, A. Golitschek, C. Koutsimanis, and X. Shen, "Relaying operation in 3GPP LTE: Challenges and solutions," *IEEE Commun. Mag.*, vol. 50, no. 2, pp. 156–162, June 2012.

[2] B. Rankov and A. Wittneben, "Spectral efficient protocols for half-duplex fading relay channels," *IEEE J. Sel. Areas Commun.*, vol. 25, no. 2, pp. 379–389, Feb. 2007.

[3] R. H. Y. Louie, Y. Li, and B. Vucetic, "Practical physical layer network coding for two-way relay channels: Performance analysis and comparison," *IEEE Trans. Wireless Commun.*, vol. 9, no. 2, pp. 764–777, Feb. 2010.

[4] S. J. Kim, N. Devroye, P. Mitran, and V. Tarokh, "Achievable rate regions and performance comparison of half duplex bi-directional relaying protocols," *IEEE Trans. Inf. Theory*, vol. 57, no. 10, pp. 6405–6418, Oct. 2011.

[5] M. Hasna and M.-S. Alouini, "A performance study of dual-hop transmissions with fixed gain relays," *IEEE Trans. Wireless Commun.*, vol. 3, no. 6, pp. 1963–1968, Nov. 2004.

[6] J. Laneman, D. N. C. Tse, and G. W. Wornell, "Cooperative diversity in wireless networks: Efficient protocols and outage behavior," *IEEE Trans. Inf. Theory*, vol. 50, no. 12, pp. 3062–3080, Dec. 2004.

[7] N. C. Beaulieu and S. S. Soliman, "Exact analysis of multihop amplify-and-forward relaying systems over general fading links," *IEEE Trans. Commun.*, vol. 60, no. 8, pp. 2123–2134, Aug. 2012.

[8] S. Ikki and S. Aïssa, "Performance analysis of amplify-and-forward relaying over Weibull-fading channels with multiple antennas," *IET Commun.*, vol. 6, no. 2, pp. 165–171, Jan. 2012.

[9] T. Schenk, *RF Imperfections in High-Rate Wireless Systems: Impact and Digital Compensation*. Springer Netherlands, 2008.

[10] J. Qi, S. Aïssa, and M.-S. Alouini, "Analysis and compensation of I/Q imbalance in amplify-and-forward cooperative systems," in *Proc. IEEE Wireless Commun. Netw. Conf. (WCNC)*, Apr. 2012, pp. 215–220.

[11] M. Mokhtar, A. Gomaa, and N. Al-Dhahir, "OFDM AF relaying under I/Q imbalance: Performance analysis and baseband compensation," *IEEE Trans. Commun.*, vol. 61, no. 4, pp. 1304–1313, Apr. 2013.

[12] J. Qi, S. Aïssa, and M.-S. Alouini, "Multi-hop amplify-and-forward relaying cooperation in the presence of I/Q imbalance," in *Proc. IEEE Int. Conf. Commun. (ICC)*, June 2013, pp. 4978–4982.

[13] J. Li, M. Matthaiou, and T. Svensson, "I/Q imbalance in AF dual-hop relaying: Performance analysis in Nakagami-$m$ fading," *IEEE Trans. Commun.*, vol. 62, no. 3, pp. 836–847, Mar. 2014.

[14] J. Qi, S. Aïssa, and M.-S. Alouini, "Impact of I/Q imbalance on the performance of two-way CSI-assisted AF relaying," in *Proc. IEEE Wireless Commun. Netw. Conf. (WCNC)*, Apr. 2013, pp. 2507–2512.

[15] J. Li, M. Matthaiou, and T. Svensson, "I/Q imbalance in two-way AF relaying: Power allocation and performance analysis," in *Proc. IEEE Int. Conf. Commun. (ICC)*, June 2014.

[16] ——, "I/Q imbalance in two-way AF relaying," *to appear IEEE Trans. Commun.*, 2014.

[17] M. Valkama, M. Renfors, and V. Koivunen, "Advanced methods for I/Q imbalance compensation in communication receivers," *IEEE Trans. Signal Process.*, vol. 49, no. 10, pp. 2335–2344, Oct. 2001.

[18] B. Maham, O. Tirkkonen, and A. Hjørungnes, "Impact of transceiver I/Q imbalance on transmit diversity of beamforming OFDM systems," *IEEE Trans. Commun.*, vol. 60, no. 3, pp. 643–648, Mar. 2012.

[19] Ö. Özdemir, R. Hamila, and N. Al-Dhahir, "I/Q imbalance in multiple beamforming OFDM transceivers: SINR analysis and digital baseband compensation," *IEEE Trans. Commun.*, vol. 61, no. 5, pp. 1914–1925, May 2013.

[20] J. Qi and S. Aïssa, "Analysis and compensation of I/Q imbalance in MIMO transmit-receive diversity systems," *IEEE Trans. Commun.*, vol. 58, no. 5, pp. 1546–1556, May 2010.

[21] D. Tse and P. Viswanath, *Fundamentals of Wireless Communication*. Cambridge University Press, 2005.

[22] E. G. Larsson, "MIMO detection methods: How they work [lecture notes]," *IEEE Signal Processing Mag.*, vol. 26, no. 3, pp. 91–95, May 2009.

[23] E. Björnson, M. Matthaiou, and M. Debbah, "A new look at dual-hop relaying: Performance limits with hardware impairments," *IEEE Trans. Commun.*, vol. 61, no. 11, pp. 4512–4525, Nov. 2013.

[24] M. Matthaiou, A. Papadogiannis, E. Björnson, and M. Debbah, "Two-way relaying under the presence of relay transceiver hardware impairments," *IEEE Commun. Lett.*, vol. 17, no. 6, pp. 1136–1139, June 2013.